OXFORD

Human Molecular Genetics, 2020, Vol. 29, No. 8 1340–1352

https://doi.org/10.1093/hmg/ddaa061
Advance Access Publication Date: 2 April 2020
General Article

GENERAL ARTICLE

Nemo-like kinase reduces mutant huntingtin levels and mitigates Huntington's disease

Mali Jiang[1], Xiaoyan Zhang[1], Hongshuai Liu[1], Jared LeBron[1], Athanasios Alexandris[1,†], Qi Peng[1], Hao Gu[1], Fanghan Yang[1], Yuchen Li[1], Ruiling Wang[1], Zhipeng Hou[2], Nicolas Arbez[1], Qianwei Ren[1], Jen-Li Dong[1], Emma Whela[1], Ronald Wang[1], Tamara Ratovitski[1], Juan C. Troncoso[3], Susumu Mori[2], Christopher A. Ross[1,4,5,6], Janghoo Lim[7] and Wenzhen Duan[1,4,8,*]

[1]Division of Neurobiology, Department of Psychiatry and Behavioral Sciences, Johns Hopkins University School of Medicine, Baltimore, MD, USA, [2]Department of Radiology, Johns Hopkins University School of Medicine, Baltimore, MD, USA, [3]Division of Neuropathology, Department of Pathology, Johns Hopkins University School of Medicine, Baltimore, MD, USA, [4]Department of Neuroscience, Johns Hopkins University School of Medicine, Baltimore, MD, USA, [5]Department of Pharmacology and Molecular Sciences, Johns Hopkins University School of Medicine, Baltimore, MD, USA, [6]Department of Neurology, Johns Hopkins University School of Medicine, Baltimore, MD, USA, [7]Departments of Genetics and of Neuroscience, Yale University School of Medicine, New Haven, CT, USA and [8]Program in Cellular and Molecular Medicine, Johns Hopkins University School of Medicine, Baltimore, MD, USA

*To whom correspondence should be addressed at: Division of Neurobiology, Department of Psychiatry and Behavioral Sciences, Johns Hopkins University School of Medicine, CMSC 8-121, 600 North Wolfe Street, Baltimore, MD 21287, USA. Tel: 410-502-2866; Fax: 410-614-0013; Email: wduan2@jhmi.edu

Abstract

Nemo-like kinase (NLK), an evolutionarily conserved serine/threonine kinase, is highly expressed in the brain, but its function in the adult brain remains not well understood. In this study, we identify NLK as an interactor of huntingtin protein (HTT). We report that NLK levels are significantly decreased in HD human brain and HD models. Importantly, overexpression of NLK in the striatum attenuates brain atrophy, preserves striatal DARPP32 levels and reduces mutant HTT (mHTT) aggregation in HD mice. In contrast, genetic reduction of NLK exacerbates brain atrophy and loss of DARPP32 in HD mice. Moreover, we demonstrate that NLK lowers mHTT levels in a kinase activity-dependent manner, while having no significant effect on normal HTT protein levels in mouse striatal cells, human cells and HD mouse models. The NLK-mediated lowering of mHTT is associated with enhanced phosphorylation of mHTT. Phosphorylation defective mutation of serine at amino acid 120 (S120) abolishes the mHTT-lowering effect of NLK, suggesting that S120 phosphorylation is an important step in the NLK-mediated lowering of mHTT. A further mechanistic study suggests that NLK promotes mHTT ubiquitination and degradation via the proteasome pathway. Taken together, our results indicate a protective role of NLK in HD and reveal a new molecular target to reduce mHTT levels.

[†]Athanasios Alexandris, http://orcid.org/0000-0002-5324-8355

Received: January 28, 2020. **Revised:** March 15, 2020. **Accepted:** March 30, 2020

Introduction

HD is caused by the mutation in the *huntingtin* (*HTT*) gene, which encodes the mutant huntingtin protein (mHTT) with an expanded polyglutamine tract (polyQ) (1). The gain of toxic function of mHTT is the major cause of HD, though molecular mechanisms remain elusive and likely involve multiple pathways that are highly challenging to target simultaneously (2,3). Although a recent GWAS in HD subjects reported that the onset of HD is determined by non-interrupted CAG repeat length rather than polyQ length, as authors indicated, the data do not reveal what drives the resultant cellular toxicity and do not exclude an effect of polyQ on mHTT toxicity (4). In fact, it has been widely demonstrated that nearly all pathological mechanisms are driven by the presence of the mHTT, and reducing mHTT protein accumulation or increasing its clearance has proven to be beneficial in HD (5,6). Lowering mHTT may provide an effective approach in treating HD by ameliorating its downstream toxicity. If successful, this strategy may modify disease progression in human HD. In fact, non-allele-specific lowering of HTT levels by a variety of genetic approaches has been shown to effectively mitigate mHTT toxicity in HD models and would be a promising therapeutic approach for HD patients with recent clinical trials (7).

However, genetic approaches such as RNA interference (RNAi), zinc finger protein (ZFP), CRISPR/Cas9 or antisense oligonucleotides (ASOs) still face challenges in effective delivery to all affected brain regions of HD patients, particularly given the long duration of natural HD progression (8). Because normal HTT is an essential protein during development (9,10) and may play a protective role in HD (11), lowering normal HTT to an intolerable extent may have a harmful impact, particularly in long-term treatment (9). Therefore, identifying a molecular target that has the potential to selectively lower mHTT could be highly valuable for the development of HD treatment. In addition, developing potential therapies for HD is particularly feasible because HD is a genetically homogeneous disease with numerous well-established animal and cell-based models (12,13).

mHTT is prone to aggregate and form inclusions in neurons, particularly in selectively vulnerable brain regions in HD like the striatum and cerebral cortex, indicating that the protein clearance system is impaired in HD (14–16). Cellular mechanisms promoting mHTT clearance are of great interest because they can lower the levels of the mHTT protein and its toxic species, thus affecting HD progression (17–20). Although the CAG repeat length is a major determining factor in the onset and neuropathological severity of HD, other disease modifiers have recently been identified (21,22), suggesting that HD onset and progression are both modifiable.

mHTT degradation is mediated by two major protein clearance systems: the ubiquitin–proteasome system (UPS) and autophagy–lysosomal pathway (23,24). These two systems coordinate to degrade misfolded or unfolded proteins and protein aggregates (25,26). mHTT has been associated with dysfunction in both the UPS and the autophagy–lysosomal pathway (27,28). Interestingly, ubiquitination can direct HTT for clearance via both pathways (29).

Nemo-like kinase (NLK) is an evolutionarily conserved serine/threonine kinase and plays a role in multiple processes due to its capacity to regulate a diverse array of downstream signaling pathways (30). Although NLK is known to be expressed at high levels in the nervous system, its function in the adult brain is not well understood. It has been reported that NLK interacts with two other polyQ containing disease-causing proteins, Ataxin1 (ATXN1) and androgen receptor (AR) (31,32). PolyQ expansion in the ATXN1 and AR proteins causes spinocerebellar ataxia type 1 (SCA1) and spinal and bulbar muscular atrophy (SMBA), respectively, and genetic reduction of NLK levels modulates behavioral deficits and neuropathology in both SCA1 and SBMA models (31,32). In addition, a previous mass spectrometry screening study implicates a potential interaction between NLK and mHTT (33).

In this study, we identify that NLK interacts with both wild-type and mutant forms of endogenous HTT protein. We show that NLK levels are significantly decreased in HD brain and HD models. Importantly, overexpression of NLK in the striatum attenuates HD neuropathology, whereas genetic reduction of NLK levels exacerbates the HD neuropathology. Furthermore, we demonstrate that NLK lowers mHTT levels in mouse striatal cells and mouse models of HD. This mHTT-lowering effect of NLK is associated with HTT phosphorylation at S120. The mechanistic data suggest that NLK promotes mHTT ubiquitination and degradation via the proteasome pathway. Our preclinical data support a protective role of NLK in HD and reveal a novel molecular target that can specifically decrease mHTT levels.

Results

HTT interacts with NLK

A mass spectrometry screen of HTT interactors suggests a potential interaction between mHTT and NLK (peptide) (33). To determine whether HTT physically interacts with NLK, HEK293-FT cells were co-transfected with Flag-NLK and full-length (FL) HTT either with 123 CAG repeats (mHTT) or 23 CAG repeats (wHTT). Cell extracts expressing mHTT or wHTT and Flag-NLK were subjected to co-immunoprecipitation (co-IP) with indicated HTT antibodies. Western blot analysis showed interaction of NLK with both wHTT and mHTT (Fig. 1A). These results support physical interaction between NLK and full-length HTT. Since N-terminal HTT is reported as the most toxic fragment, we then co-transfected Flag-NLK and Myc-N-terminal 171aa HTT with either 18Q (Myc-N-wHtt) or 82Q (Myc-N-mHTT) in HEK 293 FT cells. Co-IP experiment was performed with c-Myc monoclonal antibody. Western blot analysis revealed that both N-mHTT and N-wHTT interacted with NLK (Fig. 1B). We also found that transfected NLK and HTT were detected in both cytoplasmic and nuclear compartments (Fig. 1C).

In order to determine whether endogenous HTT interacts with NLK, a homozygous full-length *mHTT* knock-in zQ175 mouse model was used. Mouse brain samples from either wild-type (WT) littermate control or zQ175 HD mice were gently homogenized and co-immunoprecipitated with NLK antibody followed by western blot analysis with indicated HTT antibodies (Fig. 1D upper panel). Conversely, co-IP with indicated HTT antibodies and western blotting analysis with NLK antibody were performed (Fig. 1D middle panel). Our results demonstrated that both wHTT and mHTT interacted with NLK in the mouse brain. Taken together, the results confirmed an interaction between HTT protein and NLK in both co-expression in human cells as well as endogenous proteins in the mouse brain.

NLK levels are significantly decreased in HD

Because NLK interacts with mHTT, we then asked whether NLK levels are altered in HD condition. We observed that NLK levels were significantly lower in human HD postmortem brain (cortex A4, we used cortex samples because caudate/putamen almost degenerated/disappeared in human HD postmortem brain) than

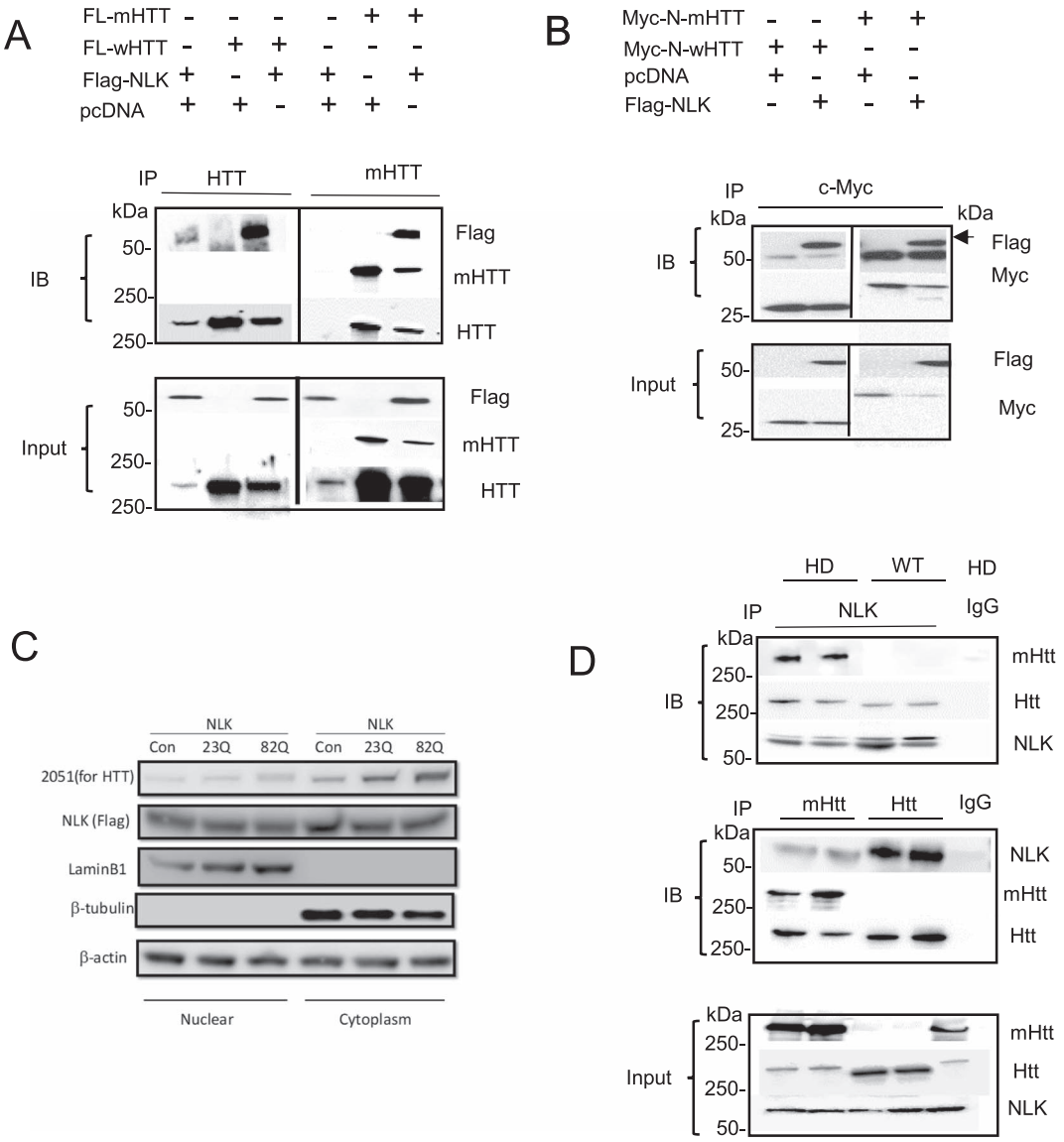

Figure 1. NLK interacts with HTT. (**A**) HEK293-FT cells were co-transfected with Flag-NLK and FL-HTT with 23Q (wHTT) or 123Q (mHTT), or pcDNA as a control. Cells were collected for immunoprecipitation (IP). Western blotting analysis was performed with MW1 antibody to mHTT, MAB2166 antibody to HTT (both wHTT and mHTT) or anti-Flag antibody (to transgene NLK). (**B**) HEK293-FT cells were co-transfected with Flag-NLK and Myc-N171-HTT with 18Q or 82Q. Cells were collected for the IP experiments. Western blotting was performed with anti c-Myc (to N-HTT) or Flag (to NLK) antibodies. Arrow indicated the specific band for Flag-NLK. (**C**) NLK and HTT are detected in both nuclear and cytoplasmic compartments. HEK293-FT cells were co-transfected with Flag-tagged NLK and full-length HTT with either 23Q or 82Q. Cell extracts from indicated groups were subject to subcellular fractionation. Nuclear fraction and cytoplasm compartment were subjected to Western blotting. Transfected HTT and NLK were expressed in both compartments. (**D**) Mouse cerebral cortex samples from 6-month-old homozygous zQ175 HD or WT mice were subjected to co-IP with anti-NLK antibody and then blotting with HTT antibodies (MW1 for mHTT, MAB 2166 for HTT). Alternatively, samples were subjected to co-IP with indicated HTT antibodies and then western blotting was performed with anti-NLK antibody.

those in age-matched controls (Fig. 2A). We further investigated NLK levels in two HD mouse models which we used for the *in vivo* study. As expected, NLK levels were also decreased in the striatum of 6-month-old N171-82Q HD mice (Fig. 2B) and 12-month-old full-length HdhQ250 knock-in mice (Fig. 2C). Furthermore, we measured NLK levels in the striatal cells expressing either full-length mHTT ($STHdh^{Q111/Q111}$) or wHTT ($STHdh^{Q7/Q7}$). This HD cell model has been widely used in HD research since its development by Dr MacDonald's group (34). $STHdh^{Q111/Q111}$ are more vulnerable to serum withdrawal than $STHdh^{Q7/Q7}$ cells, indicated by decreased ATP levels and increased LDH release in $STHdh^{Q111/Q111}$ cells at 24 h after serum withdrawal (34,35). We found that NLK levels were significantly lower in the mHTT expressing cells at 24 h after serum withdrawal (Fig. 2D). To investigate whether the reduction of HTT levels by NLK is due to an effect on HTT transcription, qRT–PCR was performed. We found that HTT mRNA levels were not significantly altered by NLK overexpression (data not shown), suggesting that NLK modulates mHTT levels at post-transcriptional level. Altogether, these findings establish that NLK levels are decreased in HD condition.

Overexpression of NLK in the striatum protects HD mice

Since NLK levels are decreased in HD, we went on to determine the role of NLK in the mouse model of HD. We have shown

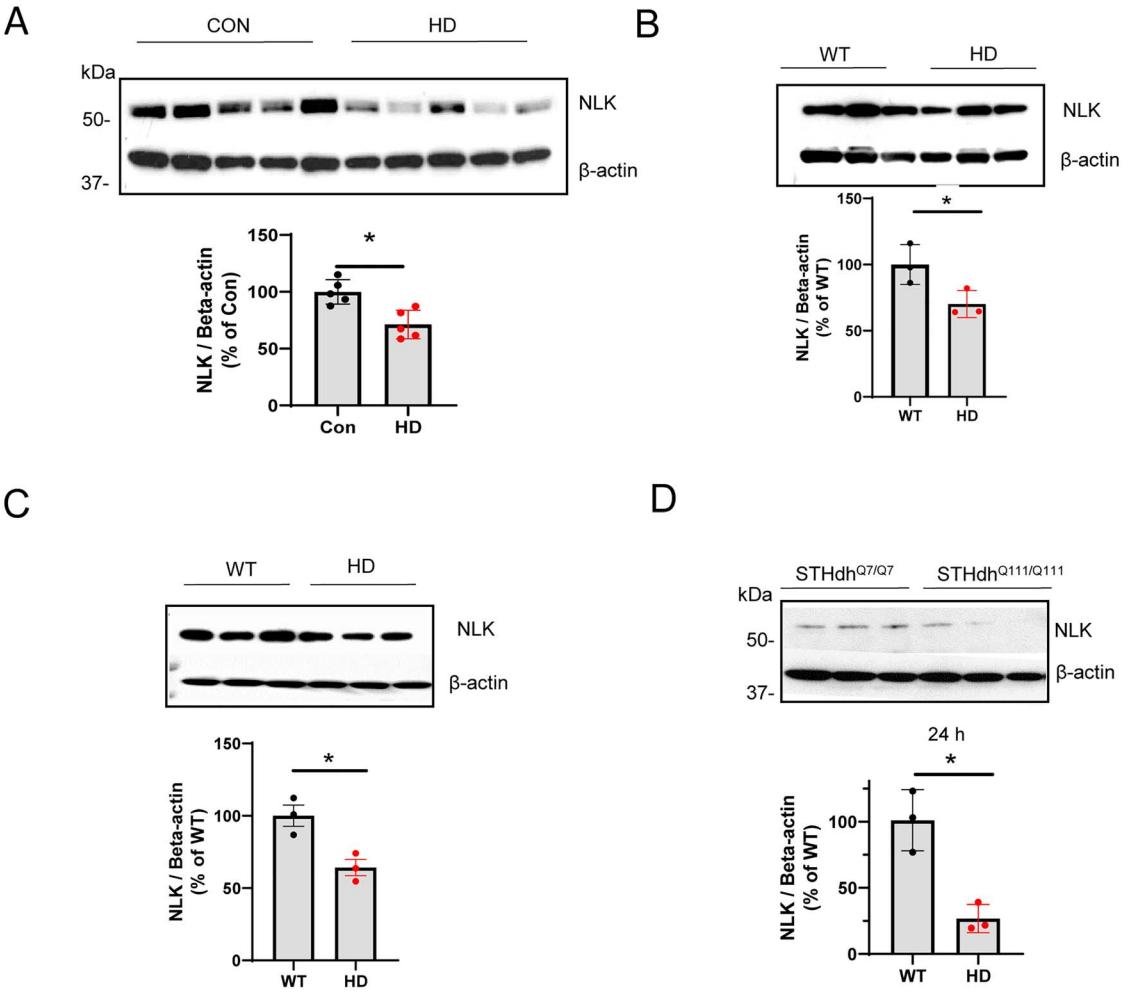

Figure 2. NLK protein levels are decreased in HD. (**A**) NLK levels in the human postmortem control (Con) and HD motor cortex A4. Western blotting was performed with NLK and β-actin antibodies. Intensity of blots was quantified by NIH Image J software and normalized by β-actin loading controls. $n = 5$. (**B**) NLK levels in the striatum of N171-82Q HD and WT mice at 6 months age. $n = 3$. (**C**) NLK levels in the striatum of HdhQ 250Q HD and WT mice at 12 months age. $n = 3$. (**D**) NLK levels in the striatal cells expressing wild type (WT, $STHdh^{Q7/Q7}$) or mHTT (HD, $STHdh^{Q111/Q111}$). The values are expressed as Mean ± SE, $^{*}P < 0.05$ between HD and control group by unpaired Student's *t*-test.

that NLK interacts with N171 HTT (Fig. 1B), a well-characterized N171-82Q HD model (36). These HD mice exhibit progressive brain atrophy, decreased dopamine- and cAMP-regulated neuronal phosphoprotein 32 (DARPP32) levels in the striatum, mHTT aggregation, impaired motor function and weight loss (36,37).

We injected AAV_2-NLK (GFP tagged) into the striatum of HD or WT mice at 10 weeks of age and evaluated the effects of NLK on HD brain pathology and phenotypes at 16 weeks of age. The successful expression of NLK in the striatal neurons was verified by GFP fluorescence (left panel) and western blotting (right panel) (Fig. 3A). As predicted, NLK expression increases in the striatum attenuated brain atrophy, indicated by the preservation of brain volumes in NLK-injected (NLK) HD mice compared to those injected with AAV_2-GFP (CON) (Fig. 3B).

HD pathology is marked by an extensive loss of medium spiny neurons in the striatum which usually express high levels of DARPP32. DARPP32 is a fundamental component of the dopamine-signaling cascade and serves as a marker of neuronal dysfunction or loss in HD when expressed at decreased levels. Consistent with its protective effect, NLK overexpression also preserved DARPP32 levels in the striatum of HD mice (Fig. 3C).

mHTT aggregation is a pathological hallmark of HD that was discovered initially in HD mice and then verified in the HD patients' brain. Thus the HD mouse models are particularly valuable in understanding HD pathogenesis (38). The N171-82Q HD mice show EM48 positive mHTT aggregates in the striatum. As predicted, NLK overexpression dramatically reduced the mHTT aggregates (Fig. 3D). Taken together, these *in vivo* findings support a neuroprotective role of NLK in HD.

Genetic reduction of NLK exacerbates neuropathology in HD mice

To evaluate the therapeutic potential of modulating NLK levels/activity, and whether reduced NLK levels is detrimental in HD, we crossed full-length heterozygous mHTT knock-in HdhQ250 mice with NLK knockout (NLK+/−) mice (31). HdhQ250 mice exhibit adult-onset progressive brain pathology (about 6 months of age) that recapitulates human HD pathology (39). Since we hypothesize that NLK reduction worsens HD pathology, this HD model is suitable to test our hypothesis. Western blot analysis confirmed that NLK levels were decreased by about 50% in NLK +/− mice compared to WT mice (NLK+/+) (Fig. 4A).

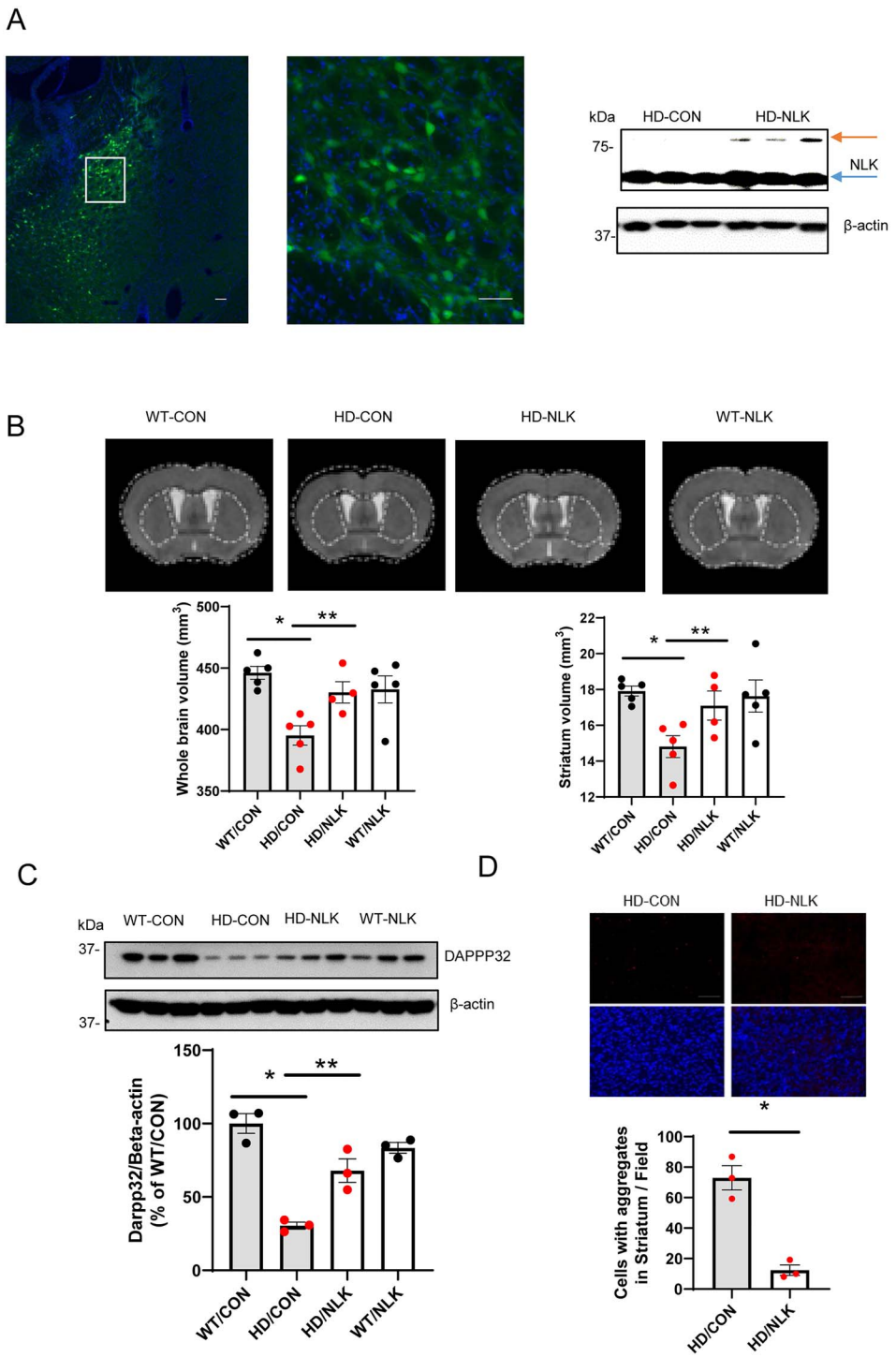

Figure 3. Overexpression of NLK attenuates brain pathology in HD mice. N171-82Q mice were injected with AAV_2-NLK or AAV_2-GFP control (CON) to the striatum at the age of 10 weeks. (**A**) Expression of AAV-mediated NLK (GFP-tagged) in the striatum was evidenced at 3 weeks after AAV injection. Scale bar is 50 μm. Western blots of striatal samples from indicated groups suggest that AAV-NLK was expressed. Note that the lower bands (blue arrow) represent the endogenous NLK (about 55KDa), and the upper bands are NLK transgene (GFP-tagged, orange arrow). (**B**) *In vivo* structural MRI was conducted at 16 weeks of age. Values are Mean ± SE, $n = 4$–5. $^{*}P < 0.05$ compared with the value of WT/CON, $^{**}P < 0.05$ compared with the value of HD by one-way *ANOVA* with Holm–Sidak post hoc test. (**C**) Representative western blot of DARPP32 and quantification data. Values are Mean ± SE, $n = 3$. $^{*}P < 0.05$ compared with the value of WT/CON, $^{**}P < 0.05$ compared with the value of HD by one-way *ANOVA* with Holm–Sidak post hoc test. (**D**) Representative images from HD mouse striatum immunostained with EM48 antibody. Scale bar is 50 μm. Number of cells with mHTT aggregates were quantified per microscope field. Mean ± SE. $n = 3$. $^{*}P < 0.05$ versus HD/CON group by unpaired Student's *t*-test.

Notably, mHTT levels (Fig. 4A) but not wHTT levels (Fig. 4B) were increased in the NLK +/− condition, suggesting that NLK specifically modulates mHTT levels. The 50% reduction of NLK exacerbated brain atrophy in HD mice without affecting WT brain volumes, indicated by the further reduction of brain volumes in HD/NLK +/− mice compared to those in HD/NLK +/+ mice (Fig. 4C). Furthermore, NLK reduction decreased DARPP32 levels in HD mice (Fig. 4D). These findings suggest that reducing NLK levels has a detrimental effect in HD brain pathology.

NLK selectively reduces mHTT levels in a kinase-dependent manner

From the *in vitro* and *in vivo* experiments presented above, we noticed that NLK specifically reduced mHTT levels (See Figs 1A and 4A). To validate the effect of NLK on mHTT levels and determine whether the kinase activity of NLK mediates such modulation, we investigated the effect of NLK on HTT levels in a mouse striatal cell model expressing endogenous levels of wHTT (Q7) or mHTT (Q111). These striatal precursor cells were derived from HTT knock-in mouse brain and have been widely used. Mouse striatal cells were transfected by lipofectamine, resulting in approximately 30% transfection efficiency (Fig. 5A). We revealed that NLK significantly reduced mHTT levels (Fig. 5B) but did not alter wHTT levels in the striatal cells (Fig. 5C) and human HEK293 cells (Fig. 5D). These findings suggest that the NLK-mediated lowering of endogenous HTT levels is mHTT-specific.

To determine whether the effects of NLK on mHTT levels are mediated by its kinase activity, the human HEK293 cells were transfected with either wild-type (NLK WT) or kinase-null NLK (NLK KN). We found that the kinase-null mutation of NLK completely abolished its mHTT-lowering effects in the human cells (Fig. 5E), suggesting that the kinase activity is a key mediator for the mHTT lowering effect of NLK.

To investigate whether the reduction of HTT levels by NLK is due to an effect on *HTT* transcription, qRT–PCR was performed. Our data indicated that *HTT* mRNA levels were not significantly altered by NLK overexpression (data not shown), suggesting that NLK modulates mHTT levels at post-transcriptional level.

The effect of NLK on mHTT levels is mediated by HTT phosphorylation at S120

Since the kinase activity of NLK mediates its mHTT-lowering effect, it is possible that mHTT is a substrate of NLK. NLK is a conserved serine/threonine kinase and functions as a proline (Pro)-directed kinase. This means that NLK phosphorylates proteins at a serine or threonine residue that is immediately preceding a proline residue (S/T-P). There are multiple S/T-P sites in both N-terminal and C-terminal of human HTT protein. To test whether NLK phosphorylates mHTT, HEK293-FT cells were co-transfected with full-length mHTT and NLK or pcDNA control. mHTT proteins were first co-immunoprecipitated with MW1 antibody (to mHTT) and then immunoblotted with either anti-HTT antibody or S/T-P phospho-specific MPM2 antibody (specific to proteins with phosphorylated S/T-P sites) to reveal total and S/T-P phosphorylated mHTT, respectively. We found that NLK expression increased phosphorylation of mHTT detected by MPM2 antibody (Fig. 6A). We consistently observed that NLK reduced mHTT levels in a kinase-dependent manner (Fig. 6B).

Because HTT contains numerous S/T-P sites, we sought to identify the potential phosphorylation site(s) in mHTT that are specifically targeted by NLK to mediate its mHTT-lowering effect. We performed an *in vitro* kinase screen using synthetic HTT peptides as substrates. We found that a peptide containing one of the N-terminal S-P sites, serine 120 (S120), was phosphorylated by NLK kinase in the *in vitro* assay (a 2.5-fold increase in the signal compared to kinase alone ± 0.04, $n = 3$). To determine whether S120 is an NLK phosphorylation site that mediates its mHTT-lowering effect, we mutated the serine at amino acid position 120 to alanine (S120A, phosphorylation-null) and examined the mHTT levels after co-transfection with NLK. We found that NLK did not reduce S120A mHTT levels (Fig. 6C), suggesting that the S120 residue phosphorylation is a key step in the reduction of mHTT levels by NLK. Furthermore, we mutated two other S-P sites at the C-terminal of mHTT, specifically S1181 and S1201, to alanine. Phosphorylation-null mutation at these two sites did not alter the NLK-mediated mHTT-lowering effect (Fig. 6D). Altogether, these findings suggest that phosphorylation of mHTT at the S120 site plays a key role in the mHTT-lowering effect of NLK.

NLK accelerates mHTT clearance via ubiquitin–proteasome system

Our results so far indicate that NLK lowers mHTT levels at the post-transcriptional level, and this effect is mediated by regulating mHTT S120 phosphorylation. To further understand the molecular mechanism involved in such mHTT-lowering effect of NLK, we examined the major protein degradation systems. There are two main systems responsible for protein clearance: The autophagy–lysosomal pathway and the ubiquitin–proteasome system (UPS). To determine which system mediates the effect of NLK on lowering mHTT levels, HEK293-FT cells were treated with either a naturally occurring selective proteasome inhibitor epoxomicin or bafilomycin A1 which inhibits autophagic flux by preventing the acidification of endosomes and autophagosome–lysosome fusion (40). Although the inhibition of UPS or autophagy pathways both increased mHTT accumulation, Epoxomicin abolished the NLK-mediated HTT-lowering effects (Fig. 7A), whereas the bafilomycin did not (Fig. 7B); this suggests that the proteasome system rather than autophagic flux pathway is the key pathway mediating the effects of NLK in reducing mHTT levels.

Ubiquitination is a post-translational modification of proteins that plays a key role in UPS-mediated protein clearance. Proteins are selectively conjugated with ubiquitin chains, which target them to proteasome for clearance. Ubiquitin is a highly conserved 76-amino acid protein that is conjugated to lysine (K) residues of target proteins by three distinct enzymes: E1 (ubiquitin-activating enzymes), E2 (ubiquitin-conjugating enzymes) and E3 (substrate-specific ubiquitin ligases). We assessed mHTT ubiquitination status by co-immunoprecipitation of mHTT with MW1 antibody and then immunoblotting with an anti-ubiquitin antibody. Our results demonstrate that NLK-transfected cells had higher levels of ubiquitinated mHTT (Fig. 7C). All together, these results suggest that NLK enhances mHTT ubiquitination and degradation via the UPS pathway.

Discussion

Approaches that reduce mHTT protein are useful in attenuating HD pathogenesis and therefore in modifying disease progression. Here we report that NLK, an evolutionarily conserved serine/threonine kinase, reduces accumulation of mHTT protein in human cells via the proteasome clearance pathway and attenuates HD-associated phenotypes in mice. Relevant to the human

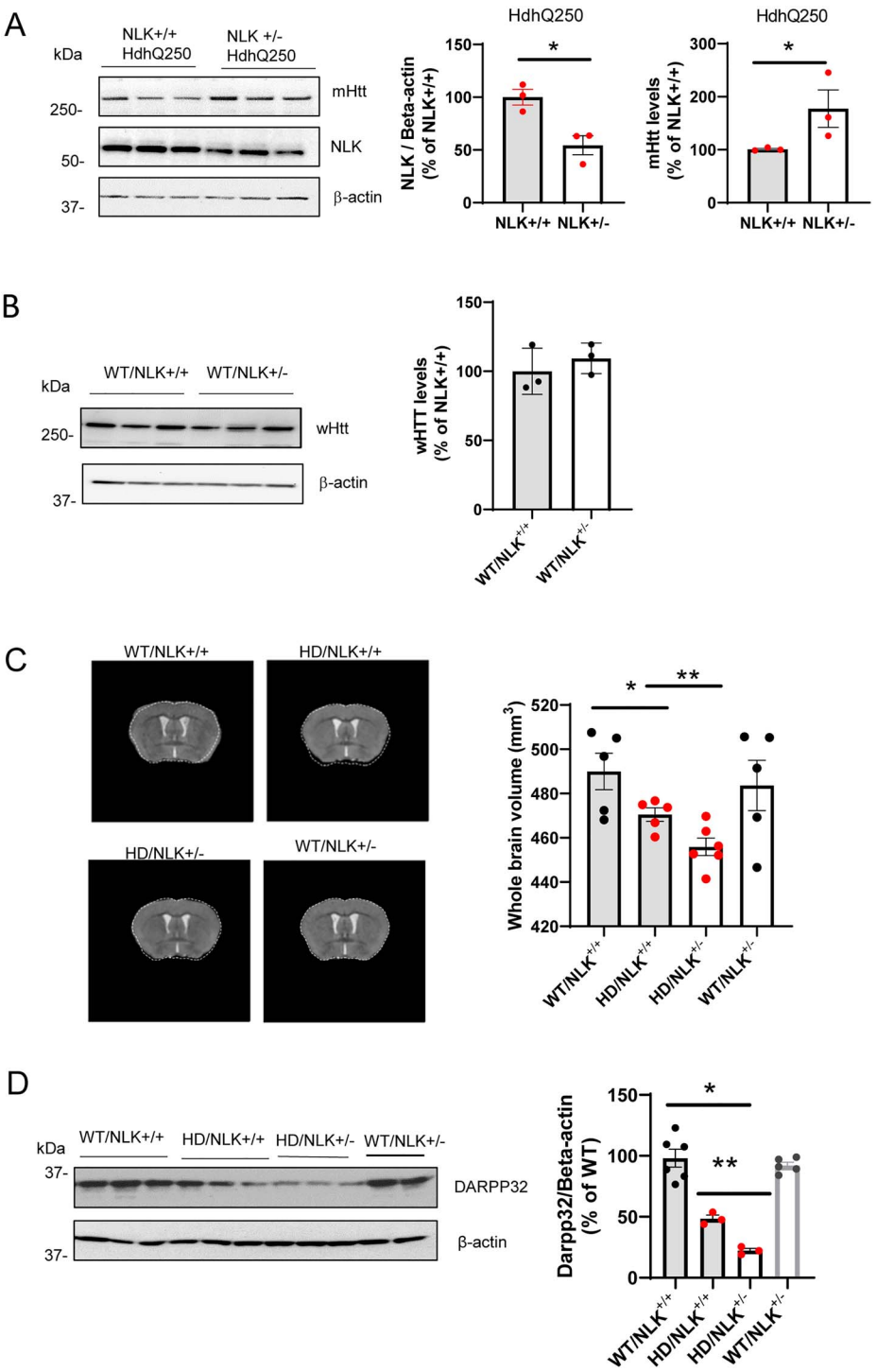

Figure 4. Reduction of NLK exacerbates brain pathology in HD mice. HdhQ250 mice were crossbred with NLKKO mice. (**A**) Reduction of NLK increases mHtt levels. HdhQ250 mice were crossbreeding with the heterozygous NLKKO mice. Western Blotting was performed with MW1 (mHtt), NLK and β-actin antibodies in the cortex of 2-month-old HD and HD/NLKKO mice. $n = 3$. The values are expressed as mean ± SE. $^{*}p < 0.05$ compared with the values of the NLK+/+ group by unpaired Student's t-test. (**B**) Reduction of NLK does not decrease wHtt levels. Western Blotting was performed with 2166 antibody in the cortex of 2-month-old WT and NLKKO mice. (**C**) Representative MRI images from indicated groups at age of 12 months (left panel). Brain volumes were determined by structural MRI (right panel). $n = 5$. (**D**) DARPP32 levels were evaluated in the striatum of 12-month-old mice. $n = 3$–6. Densitometry analysis was performed by NIH Image J. $^{*}P < 0.05$ compared with the values of the WT group, $^{**}P < 0.05$ compared with the values of the HD group by one-way *ANOVA* with Dunn's or Holm–Sidak post hoc test.

disease, we also confirm that NLK levels are decreased in HD brains. Our findings indicate that lower levels of NLK observed in HD may accelerate brain dysfunction. Our results indicate a protective role of NLK in HD and thus potentially indicate a novel target for the treatment of HD. Because NLK is highly expressed in neural tissues and minimally detected in other tissues (41), the effect of NLK activation will be primarily limited to neural tissues and thus be of great value in the development of HD therapy.

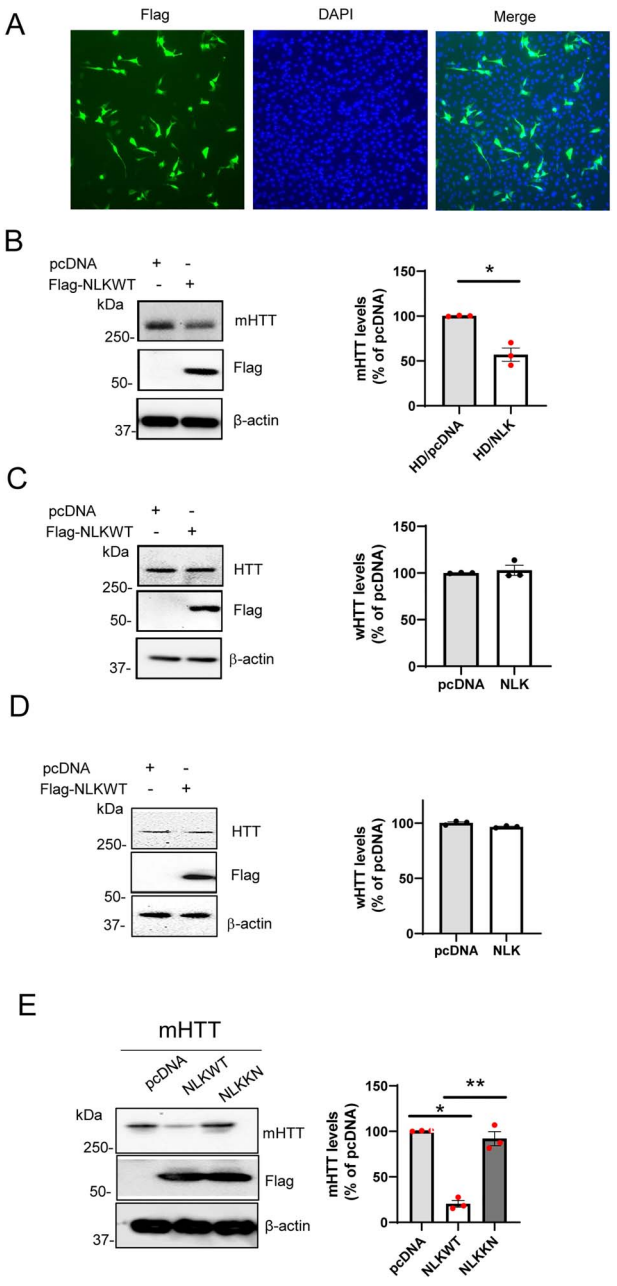

Figure 5. NLK selectively decreases endogenous mHTT protein levels in a kinase-dependent manner. (**A**) Mouse striatal precursor neurons expressing endogenous levels of mHTT (111Q) were transfected with Flag-NLK. Cells were immunostained with anti-Flag (NLK) antibody, DAPI stains nucleus. (**B**) mHTT expressing mouse striatal cells were transfected with pcDNA or NLK. Cells were collected for western blot. $n = 3$. The values are expressed as Mean ± SE. $^{*}P < 0.05$ versus HD/pcDNA group by unpaired Student's *t*-test. (**C**) Mouse striatal cells expressing wHTT (Q7) were transfected with pcDNA, or Flag-NLK. Cells were collected and western blotting was performed with MAB 2166 (HTT), Flag (NLK) and actin antibodies. $n = 3$. (**D**) Human HEK 293 cells were transfected with pcDNA or Flag-NLKWT. Cells were collected for western blot. The values are expressed as Mean ± SE, $n = 3$. (**E**) Human HEK 293 cells were co-transfected with mutant HTT (mHTT) with pcDNA or Flag-NLKWT or kinase null mutant NLK (Flag-NLK KN). Cells were collected for western blot. The values are expressed as Mean ± SE, $n = 3$. $^{*}P < 0.05$ compared with the values of the pcDNA group, $^{**}P < 0.05$ compared with the values of the NLKWT group by one-way ANOVA with Holm–Sidak post hoc test.

In the past decades, research has focused on identifying mechanisms that selectively reduce the amount of the toxic mHTT aggregates that underlie HD neurotoxicity (7,42–46). Proteasome impairment has long been deemed causative in HD (26), and studies have shown that mHTT can induce UPS impairment (24). It has been demonstrated that mHTT induces an initial impairment of the UPS which is recovered when mHTT inclusion bodies emerge (47,48). On the other hand, evidence suggests that proteasome activity decreases with age (49). Whether reduced processivity of the UPS is induced by mHTT or caused by age-related proteostasis alterations, the ameliorating effects of the UPS could be pivotal in the treatment of diseases like HD that are characterized by abnormal protein accumulations. In the present study, we analyze the role of NLK as a mediator of mHTT levels and provide a mechanism by which NLK can reduce the accumulation of mHTT protein in human cells.

In this study, we uncovered interesting mechanisms that we predict underlie the role of NLK in HD at the cellular level. First, NLK interacts with HTT at the N-terminal region of the protein (Fig. 1B). Second, NLK lowers mHTT levels in a kinase-dependent manner in human cells (Fig. 5). Third, NLK promotes the phosphorylation of mHTT at S-P sites (Fig. 6). Fourth, NLK-induced reduction of HTT levels is selective to mHTT (Fig. 5). Given that NLK promotes mHTT ubiquitination (Fig. 7), we suspect that it is acting cell autonomously to reduce mHTT levels via the proteasome system.

Of particular importance is our finding that reduction of NLK expression exacerbates the neuropathology in HD mice. However, this degree of NLK reduction does not appear to alter motor function and brain morphology in non-HD condition. As our studies were carried out using a constitutive knockdown of NLK starting from *in utero*, we cannot determine how NLK reduction exerts its effects on HD pathology if given at different stages of the disease. Future investigations using conditional NLK knockdown mice could address this question. It is important to note that NLK knockdown has been reported to rescue muscle and motor neuron pathology in SBMA and cerebellar pathology in SCA1 mouse models (31,32). The underlying molecular basis for the effects of NLK on different polyQ diseases are likely due to altered properties of specific polyQ-causing proteins by phosphorylation. For example, NLK specifically lowers mHTT levels but not the levels of the other two polyQ proteins. Moreover, NLK lowers mHTT protein levels via phosphorylation in HD, while it does not dramatically alter the expression levels of mutant ATXN1 protein by phosphorylation in SCA1. However, NLK may alter the protein toxicity of mutant ATNX1. In addition, NLK-mediated lowering of mHTT levels depends on N-terminal S120 phosphorylation rather than on the two C-terminal sites, S1181 and S1201. This specific effect of NLK on mHTT may partially, if not completely, explain its protective effect.

Therapeutic approaches that reduce both mutant and wild-type HTT in HD cells raise important concerns over the tolerance of losing wild-type HTT (50,51). Studies have suggested that loss of wild-type HTT to a certain extent in mice during embryonic and postnatal development may be harmful and lead to HD-like phenotypes (52). On the other hand, lowering wild-type HTT levels up to 60–70% has been shown to be safe in a primate model (53), and ablation of wild-type HTT in adult mice at >4 months of age does not lead to neurodegeneration or other defects (11). This suggests that lowering wild-type HTT in aged adults may be well tolerated. Encouragingly, the recently launched IONIS HTT-Rx clinical trial, by using a non-allele-specific ASO, HTTRx, for HD treatment, has demonstrated dose-dependent reductions in concentrations of mutant HTT in CSF (54). But a

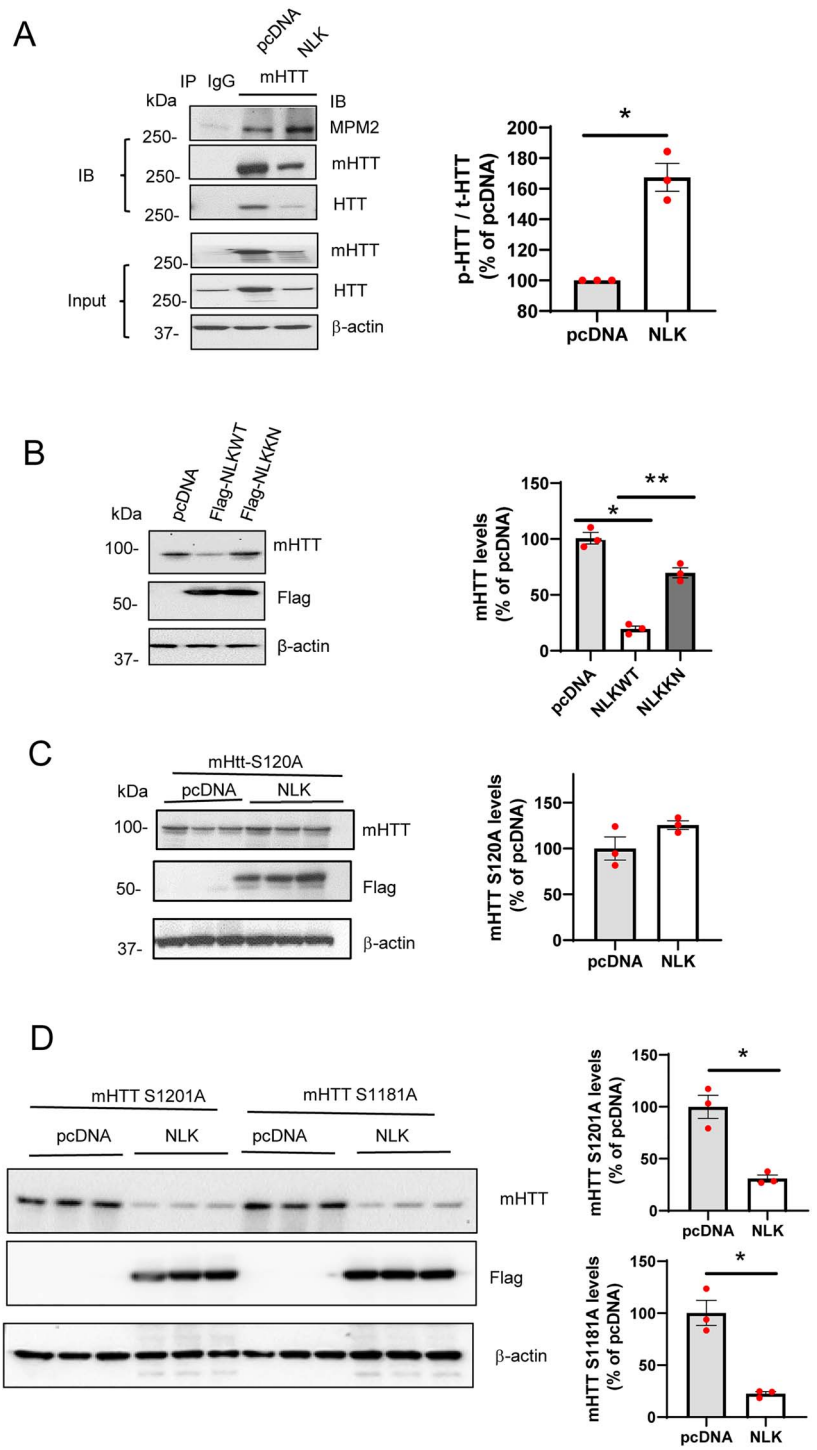

Figure 6. The effects of NLK on mHTT levels are mediated by HTT phosphorylation at S120. (**A**) NLK phosphorylates mHTT at S/T-P sites. HEK293-FT cells were co-transfected with pcDNA or Flag-NLK and full-length mHTT (123Q). Cells were collected for co-IP with mHTT antibody. Representative western blot with MPM2 (anti-phospho-S/T-P), MW1 (mHTT) and 2166 (total HTT) antibodies. The values are expressed as Mean ± SE. $n = 3$. (**B**) HEK293-FT cells were co-transfected with HTT (N586-20Q or 82Q), and Flag-NLK WT, or the kinase inactive mutant NLK-KN or pcDNA control. The values are expressed as Mean ± SE, $^{*}P < 0.05$ compared with the values of the pcDNA group, $^{**}P < 0.05$ compared with the values of the NLK-WT group by one-way ANOVA with Holm–Sidak post hoc test. (**C**) NLK had no effect on mHTT protein levels when serine 120 was mutated to alanine (S120A, phospho-resistant). HEK293-FT cells were co-transfected with pcDNA or Flag-NLK and N586-S120A mHTT, $n = 3$. (**D**) HEK293 FT cells were co-transfected with pcDNA or Flag-NLK and full-length mHTT with S1201A or S1181A mutation, and western blotting was conducted. $n = 3$. $^{*}P < 0.05$ compared with the values of the pcDNA group by unpaired Student's *t*-test.

more appealing therapeutic strategy is to use allele-specific HTT-lowering approaches to selectively reduce mHTT. When NLK was overexpressed in striatal cells, it selectively reduced mHTT levels without altering wild-type HTT levels. These selective reductions of mHTT levels were also observed in HD mouse models. We believe that the reduction of mHTT is likely to be the major mechanism that underlies the protective effect of NLK on HD-relevant phenotypes. This is strongly supported by evidence

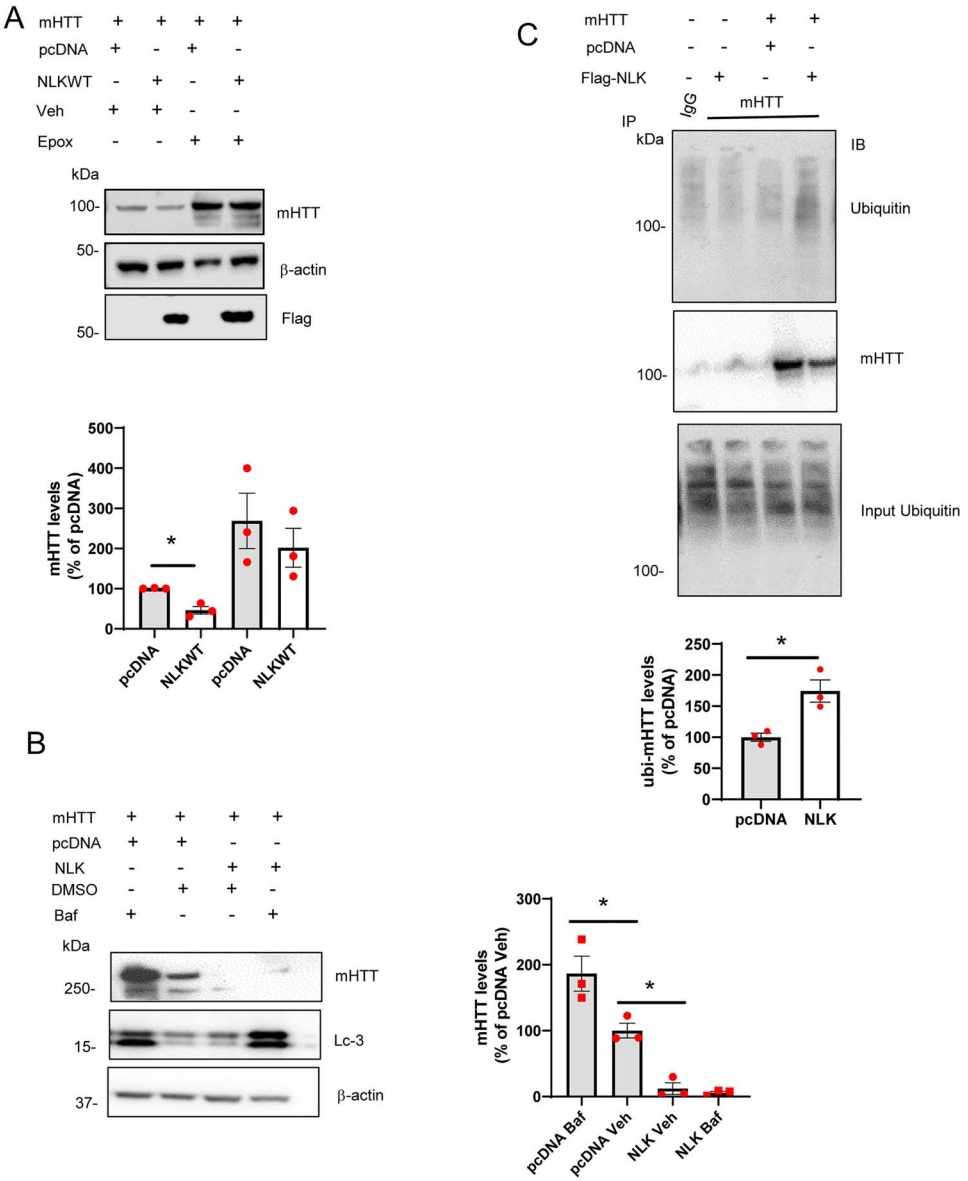

Figure 7. NLK decreases mHTT level via ubiquitin–proteasome pathway. (**A**) HEK293-FT cells were co-transfected with mHTT (N586-82Q), pcDNA, or NLK-WT for 24 h. Cells were treated with DMSO, or 50 nM epoxomicin. mHTT levels were determined at 24 h after treatment. The values are Mean ± SE. $n = 3$. $^{*}P < 0.05$ compared with the values of the pcDNA group, $^{**}P < 0.05$ compared with the values of the NLK WT group by one-way ANOVA with Holm–Sidak post hoc test. (**B**) HEK293-FT cells were co-transfected with mHTT and pcDNA or Flag-NLK. Cells were collected at 24 h after transfection for co-IP with mHTT antibody followed by western blot with anti-ubiquitin antibody. The values are Mean ± SE, $n = 3$. $^{*}P < 0.05$ compared with the values of the pcDNA group by unpaired Student's *t*-test. (**C**) HEK293-FT cells were co-transfected with mHTT and pcDNA or Flag-NLK. Cells were collected at 24 h after transfection for co-IP with mHTT antibody followed by western blot with anti-ubiquitin antibody. The values are Mean ± SE, $n = 3$. $^{*}P < 0.05$ compared with the values of the pcDNA group by unpaired Student's *t*-test.

from other approaches that rescue HD-relevant phenotypes by reducing mHTT levels, such as directly knocking down HTT (46). Our results suggest that the protective effect of NLK in HD mice is likely mediated through the lowering of mHTT. However, it is impossible to entirely exclude potential secondary effects that may have also been involved. Nevertheless, identification of NLK as a potential druggable target to lower mHTT and associated toxicity warrants its further study for HD therapy.

The accumulation of mHTT aggregates is a pathological hallmark found in the affected neurons in HD postmortem human brains as well as HD mouse brains. The NLK-mediated enhancement of mHTT ubiquitination and proteasome-mediated degradation of mHTT accelerate mHTT clearance from neurons which may lead to reduction of mHTT aggregation in the HD mouse striatum when NLK was overexpressed. We demonstrate that an increase in NLK is sufficient to reduce mHTT aggregates in the HD mouse brain. Although we have revealed a mechanistic sketch of NLK-mediated HTT regulation, further mechanistic details are yet to be identified.

Protein phosphorylation is a dynamic posttranslational modification (PTM) that allows precise temporal control of protein structure, function, subcellular localization and degradation. Phosphorylation of N-terminal serine residues of HTT has been detected in the human brain and HD models (55). However, the role of phosphorylation in regulating the structure, aggregation and HD pathology remains poorly understood,

primarily due to the lack of tools that enable site-specific and efficient modulation of phosphorylation *in vivo*. The observation that a phosphorylation-null mutation of HTT at N-terminal S120, and not at C-terminal S1181 and S1201, abolishes NLK-mediated reduction of mHTT levels provides compelling evidence for the potential role of site-specific phosphorylation in regulating mHTT levels. These results underscore the critical importance of achieving a more in-depth understanding of the effects of phosphorylation at the site-specific residues.

The development of therapeutic approaches to treat HD by reducing mHTT is an attractive avenue. Our results are an encouraging proof of principle that NLK can lower mHTT levels and improve HD brain pathology, suggesting that pharmacologically targeting NLK should be further investigated as a promising therapeutic avenue for HD treatment.

Material and Methods

Cell lines

HEK293-FT cells (ATCC) were maintained in DMEM supplemented with 10% FBS (Thermo Fisher Scientific), 0.5 mg/ml G418 (Corning Cellgro), 1% Glutamax (Thermo Fisher Scientific) and 1% penicillin/streptomycin (Gibco Thermo Fisher Scientific). Immortalized mouse striatal precursor cells with wtHTT ($STHdh^{Q7/Q7}$) or mHTT ($STHdh^{Q111/Q111}$) were purchased from Coriell Institute Cell Repository Bank (Catalog CHDI-90000071, CHDI-9000073). These cells were maintained at 33°C in high-glucose DMEM medium (Gibco, catalog 11965-118) with 10% fetal bovine serum (FBS), 1% penicillin–streptomycin, 1% L-glutamate and 400 µg/ml of G418, in a humidified atmosphere of 95% air: 5% CO_2.

Human brain tissues and HD mouse models

All procedures were conducted in strict compliance with the guide for the Animal Care and Use Committee of Johns Hopkins University and Institutional Guidelines. zQ175 mice were purchased from Jackson Laboratories (Stock number #027410) on a C57BL/6J background. Genotyping and CAG repeat size determination were conducted at Laragen Inc. (Culver City, CA, USA) by PCR. The CAG repeat length was 193 ± 7 in zQ175 mice. N171-82Q HD mice expressing N-terminal fragment HTT with 82 polyglutamine repeat were maintained on C3B6F1 background (Taconic). Male N171-82Q mice were used in our studies because of gender-dependent phenotypic differences in these HD mice (56). N171-82Q HD or littermate wild-type (WT) mice were randomly distributed to different groups. AAV_2-NLK or GFP control was injected into the striatum of mice at the age of 10 weeks. HdhQ250 mice were produced as described previously (39). Both male and female mice were used. NLK knockout (KO) mice were generated and backcrossed onto pure C57BL/6J background (31). The CAG repeat length of HdhQ250 mice used in this study was 250 ± 10. All postmortem human tissues were obtained from the Johns Hopkins Neuropathology brain bank.

NLK transfection

Lipofectamine 2000 (Invitrogen) was used to express exogenous cDNA in human HEK293-FT cells. 2 µg plasmid DNA and 4 µl lipofectamine/well were mixed. Cells were collected for western blotting, RNA extraction or immunoprecipitation (IP) at 24 h after transfection. Third generation electroporation method (Celetrix Biotechnologies) was employed for NLK transfection in mouse striatal cells. This new electroporator utilizes tubes instead of cuvettes to increase efficiency and decrease the cell damage during transfection (57). 10 µg DNA/per 2×10^6 cells and 640 V were used for each transfection.

Immunoprecipitation, western blot and subcellular fractionation

HEK293-FT cells or mouse striatal tissue were lysed in RIPA buffer (Cell Signaling) and pre-washed with Protein G Sepharose® 4 Fast Flow (GE) for 1 h. NLK or HTT were co-immunoprecipitated using anti-NLK (1:1000, Abcam), MW1 (recognizing HTT, Developmental Studies Hybridoma bank) or MAB-2166 (Millipore) antibodies for 12 h, then incubated with Protein G Sepharose® 4 Fast Flow for 2 h and washed extensively with RIPA buffer and PBS before elution. Solubilized proteins were separated by SDS–PAGE and transferred to a PVDF membrane. The membrane was incubated with primary antibodies (MW1, 1:500; MAB2166, 1:1000; NLK, 1:1000; DARPP32, 1:2000, Flag, 1:2000; β-actin, 1:5000; c-Myc 1:1000; MPM2, 1:1000; Ubiquitin, 1:1000; LC3, 1:1000; MCA 2051, 1:1000). The PVDF membrane was then exposed for 1 h to HRP-conjugated secondary antibody (1:3000; Amersham Corp), and proteins were visualized by using a chemiluminescence-based detection kit (Supersignal West Femto, Thermo Fisher Scientific). Cytoplasmic and nuclear fractions were prepared using NE-PER Nuclear and Cytoplasmic Extraction Kit (Thermo Fisher Scientific) according to the manufacturer's protocol. Nuclear marker LaminB1 (1:1000, CalbioChem) and cytosol marker beta-tubulin (1:1000, Snata cruz) were used to indicate the purity of these subcellular fractions.

In vivo structural MRI acquisition and quantification

In vivo structural MRI studies were performed on a horizontal 9.4 T magnetic resonance imager (Bruker Biospin, Billerica) with a triple-axis gradient and an animal imaging probe. The detailed image capture and analysis were described in our previous study (36). The intensity-normalized images were submitted by the Diffeomap software to a Linux cluster, which runs Large Deformation Diffeomorphic Metric Mapping (LDDMM). The transformations encode morphological differences between subject and template images and can be analyzed with deformation-based morphometry to detect regional changes in brain volume.

Stereotaxic injection

All mice were injected bilaterally into the striatum using the stereotaxic coordinates: 0.62 mm rostral to bregma, ±1.75 mm lateral to midline and 3.5 mm ventral to the skull surface. N171-82Q mice and WT littermates were injected with 4 µl of AAV_2-NLK(GFP-tagged) or AAV_2-GFP (injection rates: 0.2 µl/min) at 10 weeks of age.

Mutant HTT aggregate immunostaining

Mice were perfused and fixed by 4% paraformaldehyde. Brain sections were cut at 40 mm thickness and immunostained with an EM48 antibody (1:20, Millipore), which preferentially recognizes mutant HTT aggregates. Images were taken using Keyence BZ-X700 All-in-one Florescence microscope, and the percentage of cells with mutant HTT aggregates was calculated.

Statistics

All data are presented as mean ± SEM. SigmaStat 14.0 was used to perform all statistical analyses. We first determined the normal distribution of data by using Shapiro–Wilk normality test.

For normally distributed data, statistical significance was determined by the unpaired Student's *t*-test between two groups and one-way *ANOVA* with Holm–Sidak post hoc tests among multiple groups. For non-normal distributed data, the non-parametric Mann–Whitney test was used for two-group comparison, while one-way *ANOVA* followed by the non-parametric Dunn's multiple comparison test was used when more than two groups were compared. Differences were considered statistically significant at $P < 0.05$.

FUNDING

This research was supported by NIH grants R01NS082338 (W.D), R21NS094886 (W.D), R21NS099670 (W.D.), R01NS083706 (J.L.), R01NS088321 (J.L.) and R21MH119803 (J.L.).

Conflict of Interest Statement: The authors declared no conflict of interest.

References

1. The Huntington's Disease Collaborative Research Group (1993) A novel gene containing a trinucleotide repeat that is expanded and unstable on Huntington's disease chromosomes. *Cell*, **72**, 971–983.
2. Miller, J., Arrasate, M., Brooks, E., Libeu, C.P., Legleiter, J., Hatters, D., Curtis, J., Cheung, K., Krishnan, P., Mitra, S. *et al.* (2011) Identifying polyglutamine protein species in situ that best predict neurodegeneration. *Nat. Chem. Biol.*, **7**, 925–934.
3. Lu, B. and Palacino, J. (2013) A novel human embryonic stem cell-derived Huntington's disease neuronal model exhibits mutant huntingtin (mHTT) aggregates and soluble mHTT-dependent neurodegeneration. *FASEB J.*, **27**, 1820–1829.
4. Genetic Modifiers of Huntington's Disease Consortium. Electronic address, g.h.m.h.e. and Genetic Modifiers of Huntington's Disease, C (2019) CAG repeat not Polyglutamine length determines timing of Huntington's disease onset. *Cell*, **178**, 887–900 e814.
5. Wanker, E.E., Ast, A., Schindler, F., Trepte, P. and Schnoegl, S. (2019) The pathobiology of perturbed mutant huntingtin protein-protein interactions in Huntington's disease. *J. Neurochem.*, **151**, 507–519.
6. Aron, R., Pellegrini, P., Green, E.W., Maddison, D.C., Opoku-Nsiah, K., Wong, J.S., Daub, A.C., Giorgini, F. and Finkbeiner, S. (2018) Deubiquitinase Usp12 functions noncatalytically to induce autophagy and confer neuroprotection in models of Huntington's disease. *Nat. Commun.*, **9**, 3191.
7. Tabrizi, S.J., Ghosh, R. and Leavitt, B.R. (2019) Huntingtin lowering strategies for disease modification in Huntington's disease. *Neuron*, **102**, 899.
8. Caron, N.S., Dorsey, E.R. and Hayden, M.R. (2018) Therapeutic approaches to Huntington disease: from the bench to the clinic. *Nat. Rev. Drug Discov.*, **17**, 729–750.
9. Dragatsis, I., Levine, M.S. and Zeitlin, S. (2000) Inactivation of Hdh in the brain and testis results in progressive neurodegeneration and sterility in mice. *Nat. Genet.*, **26**, 300–306.
10. Arteaga-Bracho, E.E., Gulinello, M., Winchester, M.L., Pichamoorthy, N., Petronglo, J.R., Zambrano, A.D., Inocencio, J., De Jesus, C.D., Louie, J.O., Gokhan, S. *et al.* (2016) Postnatal and adult consequences of loss of huntingtin during development: implications for Huntington's disease. *Neurobiol. Dis.*, **96**, 144–155.
11. Wang, G., Liu, X., Gaertig, M.A., Li, S. and Li, X.J. (2016) Ablation of huntingtin in adult neurons is nondeleterious but its depletion in young mice causes acute pancreatitis. *Proc. Natl. Acad. Sci. U. S. A.*, **113**, 3359–3364.
12. Crook, Z.R. and Housman, D. (2011) Huntington's disease: can mice lead the way to treatment? *Neuron*, **69**, 423–435.
13. Szlachcic, W.J., Wiatr, K., Trzeciak, M., Figlerowicz, M. and Figiel, M. (2017) The generation of mouse and human Huntington disease iPS cells suitable for in vitro studies on Huntingtin function. *Front Mol Neurosci*, **10**, 253.
14. Krainc, D. (2010) Clearance of mutant proteins as a therapeutic target in neurodegenerative diseases. *Arch. Neurol.*, **67**, 388–392.
15. Zhao, T., Hong, Y., Li, X.J. and Li, S.H. (2016) Subcellular clearance and accumulation of Huntington disease protein: a mini-review. *Front Mol Neurosci*, **9**, 27.
16. Sarkar, S., Ravikumar, B., Floto, R.A. and Rubinsztein, D.C. (2009) Rapamycin and mTOR-independent autophagy inducers ameliorate toxicity of polyglutamine-expanded huntingtin and related proteinopathies. *Cell Death Differ.*, **16**, 46–56.
17. Ravikumar, B., Sarkar, S. and Rubinsztein, D.C. (2008) Clearance of mutant aggregate-prone proteins by autophagy. *Methods Mol. Biol.*, **445**, 195–211.
18. Harris, H. and Rubinsztein, D.C. (2011) Control of autophagy as a therapy for neurodegenerative disease. *Nat. Rev. Neurol.*, **8**, 108–117.
19. Luis-Ravelo, D., Estevez-Silva, H., Barroso-Chinea, P., Afonso-Oramas, D., Salas-Hernandez, J., Rodriguez-Nunez, J., Acevedo-Arozena, A., Marcellino, D. and Gonzalez-Hernandez, T. (2018) Pramipexole reduces soluble mutant huntingtin and protects striatal neurons through dopamine D3 receptors in a genetic model of Huntington's disease. *Exp. Neurol.*, **299**, 137–147.
20. Carnemolla, A., Michelazzi, S. and Agostoni, E. (2017) PIN1 modulates Huntingtin levels and aggregate accumulation: an in vitro model. *Front. Cell. Neurosci.*, **11**, 121.
21. Holmans, P.A., Massey, T.H. and Jones, L. (2017) Genetic modifiers of Mendelian disease: Huntington's disease and the trinucleotide repeat disorders. *Hum. Mol. Genet.*, **26**, R83–R90.
22. Genetic Modifiers of Huntington's Disease, C (2015) Identification of genetic factors that modify clinical onset of Huntington's disease. *Cell*, **162**, 516–526.
23. Lim, J. and Yue, Z. (2015) Neuronal aggregates: formation, clearance, and spreading. *Dev. Cell*, **32**, 491–501.
24. Ortega, Z. and Lucas, J.J. (2014) Ubiquitin-proteasome system involvement in Huntington's disease. *Front Mol Neurosci*, **7**, 77.
25. Li, X.J. and Li, S. (2011) Proteasomal dysfunction in aging and Huntington disease. *Neurobiol. Dis.*, **43**, 4–8.
26. Finkbeiner, S. and Mitra, S. (2008) The ubiquitin-proteasome pathway in Huntington's disease. *Scientific World Journal*, **8**, 421–433.
27. Croce, K.R. and Yamamoto, A. (2019) A role for autophagy in Huntington's disease. *Neurobiol. Dis.*, **122**, 16–22.
28. Scrivo, A., Bourdenx, M., Pampliega, O. and Cuervo, A.M. (2018) Selective autophagy as a potential therapeutic target for neurodegenerative disorders. *Lancet Neurol.*, **17**, 802–815.
29. Thompson, L.M., Aiken, C.T., Kaltenbach, L.S., Agrawal, N., Illes, K., Khoshnan, A., Martinez-Vincente, M., Arrasate, M., O'Rourke, J.G., Khashwji, H. *et al.* (2009) IKK phosphorylates Huntingtin and targets it for degradation by the proteasome and lysosome. *J. Cell Biol.*, **187**, 1083–1099.

30. Ishitani, T. and Ishitani, S. (2013) Nemo-like kinase, a multifaceted cell signaling regulator. *Cell. Signal.*, **25**, 190–197.
31. Todd, T.W., Kokubu, H., Miranda, H.C., Cortes, C.J., La Spada, A.R. and Lim, J. (2015) Nemo-like kinase is a novel regulator of spinal and bulbar muscular atrophy. *Elife*, **4**, e08493.
32. Ju, H., Kokubu, H., Todd, T.W., Kahle, J.J., Kim, S., Richman, R., Chirala, K., Orr, H.T., Zoghbi, H.Y. and Lim, J. (2013) Polyglutamine disease toxicity is regulated by Nemo-like kinase in spinocerebellar ataxia type 1. *J. Neurosci.*, **33**, 9328–9336.
33. Shirasaki, D.I., Greiner, E.R., Al-Ramahi, I., Gray, M., Boontheung, P., Geschwind, D.H., Botas, J., Coppola, G., Horvath, S., Loo, J.A. *et al.* (2012) Network organization of the huntingtin proteomic interactome in mammalian brain. *Neuron*, **75**, 41–57.
34. Trettel, F., Rigamonti, D., Hilditch-Maguire, P., Wheeler, V.C., Sharp, A.H., Persichetti, F., Cattaneo, E. and MacDonald, M.E. (2000) Dominant phenotypes produced by the HD mutation in STHdh(Q111) striatal cells. *Hum. Mol. Genet.*, **9**, 2799–2809.
35. Jin, J., Gu, H., Anders, N.M., Ren, T., Jiang, M., Tao, M., Peng, Q., Rudek, M.A. and Duan, W. (2016) Metformin protects cells from mutant Huntingtin toxicity through activation of AMPK and modulation of mitochondrial dynamics. *Neuromolecular Med.*, **18**, 581–592.
36. Cheng, Y., Peng, Q., Hou, Z., Aggarwal, M., Zhang, J., Mori, S., Ross, C.A. and Duan, W. (2011) Structural MRI detects progressive regional brain atrophy and neuroprotective effects in N171-82Q Huntington's disease mouse model. *Neuroimage*, **56**, 1027–1034.
37. Duan, W., Peng, Q., Masuda, N., Ford, E., Tryggestad, E., Ladenheim, B., Zhao, M., Cadet, J.L., Wong, J. and Ross, C.A. (2008) Sertraline slows disease progression and increases neurogenesis in N171-82Q mouse model of Huntington's disease. *Neurobiol. Dis.*, **30**, 312–322.
38. Rubinsztein, D.C. (2002) Lessons from animal models of Huntington's disease. *Trends Genet.*, **18**, 202–209.
39. Jin, J., Peng, Q., Hou, Z., Jiang, M., Wang, X., Langseth, A.J., Tao, M., Barker, P.B., Mori, S., Bergles, D.E. *et al.* (2015) Early white matter abnormalities, progressive brain pathology and motor deficits in a novel knock-in mouse model of Huntington's disease. *Hum. Mol. Genet.*, **24**, 2508–2527.
40. Mauvezin, C. and Neufeld, T.P. (2015) Bafilomycin A1 disrupts autophagic flux by inhibiting both V-ATPase-dependent acidification and Ca-P60A/SERCA-dependent autophagosome-lysosome fusion. *Autophagy*, **11**, 1437–1438.
41. Ohnishi, E., Goto, T., Sato, A., Kim, M.S., Iemura, S., Ishitani, T., Natsume, T., Ohnishi, J. and Shibuya, H. (2010) Nemo-like kinase, an essential effector of anterior formation, functions downstream of p38 mitogen-activated protein kinase. *Mol. Cell. Biol.*, **30**, 675–683.
42. Romo, L., Mohn, E.S. and Aronin, N. (2018) A fresh look at Huntingtin mRNA processing in Huntington's disease. *J Huntingtons Dis*, **7**, 101–108.
43. Miniarikova, J., Evers, M.M. and Konstantinova, P. (2018) Translation of MicroRNA-based Huntingtin-lowering therapies from preclinical studies to the clinic. *Mol. Ther.*, **26**, 947–962.
44. Aronin, N. and DiFiglia, M. (2014) Huntingtin-lowering strategies in Huntington's disease: antisense oligonucleotides, small RNAs, and gene editing. *Mov. Disord.*, **29**, 1455–1461.
45. Butler, D.C., McLear, J.A. and Messer, A. (2012) Engineered antibody therapies to counteract mutant huntingtin and related toxic intracellular proteins. *Prog. Neurobiol.*, **97**, 190–204.
46. Zeitler, B., Froelich, S., Marlen, K., Shivak, D.A., Yu, Q., Li, D., Pearl, J.R., Miller, J.C., Zhang, L., Paschon, D.E. *et al.* (2019) Allele-selective transcriptional repression of mutant HTT for the treatment of Huntington's disease. *Nat. Med.*, **25**, 1131–1142.
47. Her, L.S., Lin, J.Y., Fu, M.H., Chang, Y.F., Li, C.L., Tang, T.Y., Jhang, Y.L., Chang, C.Y., Shih, M.C., Cheng, P.H. *et al.* (2015) The differential profiling of ubiquitin-proteasome and autophagy Systems in Different Tissues before the onset of Huntington's disease models. *Brain Pathol.*, **25**, 481–490.
48. Ortega, Z., Diaz-Hernandez, M., Maynard, C.J., Hernandez, F., Dantuma, N.P. and Lucas, J.J. (2010) Acute polyglutamine expression in inducible mouse model unravels ubiquitin/proteasome system impairment and permanent recovery attributable to aggregate formation. *J. Neurosci.*, **30**, 3675–3688.
49. Vilchez, D., Saez, I. and Dillin, A. (2014) The role of protein clearance mechanisms in organismal ageing and age-related diseases. *Nat. Commun.*, **5**, 5659.
50. Zheng, Z. and Diamond, M.I. (2012) Huntington disease and the huntingtin protein. *Prog. Mol. Biol. Transl. Sci.*, **107**, 189–214.
51. Schulte, J. and Littleton, J.T. (2011) The biological function of the Huntingtin protein and its relevance to Huntington's disease pathology. *Curr Trends Neurol*, **5**, 65–78.
52. Kaemmerer, W.F. and Grondin, R.C. (2019) The effects of huntingtin-lowering: what do we know so far? *Degener Neurol Neuromuscul Dis*, **9**, 3–17.
53. Grondin, R., Kaytor, M.D., Ai, Y., Nelson, P.T., Thakker, D.R., Heisel, J., Weatherspoon, M.R., Blum, J.L., Burright, E.N., Zhang, Z. *et al.* (2012) Six-month partial suppression of Huntingtin is well tolerated in the adult rhesus striatum. *Brain*, **135**, 1197–1209.
54. Tabrizi, S.J., Leavitt, B.R., Landwehrmeyer, G.B., Wild, E.J., Saft, C., Barker, R.A., Blair, N.F., Craufurd, D., Priller, J., Rickards, H. *et al.* (2019) Targeting Huntingtin expression in patients with Huntington's disease. *N. Engl. J. Med.*, **380**, 2307–2316.
55. Kratter, I.H., Zahed, H., Lau, A., Tsvetkov, A.S., Daub, A.C., Weiberth, K.F., Gu, X., Saudou, F., Humbert, S., Yang, X.W. *et al.* (2016) Serine 421 regulates mutant huntingtin toxicity and clearance in mice. *J. Clin. Invest.*, **126**, 3585–3597.
56. Duan, W., Guo, Z., Jiang, H., Ware, M., Li, X.J. and Mattson, M.P. (2003) Dietary restriction normalizes glucose metabolism and BDNF levels, slows disease progression, and increases survival in huntingtin mutant mice. *Proc. Natl. Acad. Sci. U. S. A.*, **100**, 2911–2916.
57. Xu, X., Gao, D., Wang, P., Chen, J., Ruan, J., Xu, J. and Xia, X. (2018) Efficient homology-directed gene editing by CRISPR/Cas9 in human stem and primary cells using tube electroporation. *Sci. Rep.*, **8**, 11649.